doi: 10.22564/rbgf.v11i2.1143

AIRGLOW STUDIES VIA ROCKET-BORNE PHOTOMETERS IN BRAZIL

B.R. Clemesha and H. Takahashi

Instituto Nacional de Pesquisas Espaciais - INPE,
C.P. 515, 12201-970, São José dos Campos, SP, Brasil.

Since 1985 the Brazilian National Space Research Institute (INPE), together with the Aeronautics and Space Institute (IAE), has carried out a number of rocket experiments aimed at measuring mesospheric and thermospheric airglow emissions. The photometer payloads have been launched from the Barreira do Inferno, Natal (6°S, 35°W) and Alcântara (2°S, 44°W) launch sites, on SONDA II and SONDA III rockets. The emissions measured in these experiments were O_2 275 nm, OI 557.7 nm, Na D 589 nm, OI 630 nm, O_2 761.9 nm, and OH (8,3) 724.2 nm. The results of these experiments, together with simultaneous ground-based measurements by photometers, lidar, and ionospheric sounding, have been used to study excitation mechanisms and minor constituent concentrations in the upper mesosphere and lower thermosphere. This article presents a brief review of the published results of these studies.

ESTUDOS DE LUMINESCÊNCIA ATMOSFÉRICA ATRAVÉS DE FOTÔMETROS EM FOGUETES LANÇADOS NO BRASIL *Desde 1985 o Instituto Nacional de Pesquisas Espaciais (INPE), em conjunto com o Instituto de Aeronáutica e Espaço (IAE), vêm conduzindo vários experimentos a bordo de foguetes com a finalidade de investigar emissões aeroluminescentes da mesosfera e baixa termosfera. As cargas úteis fotométricas foram lançadas a partir dos centros de lançamento da Barreira do Inferno, Natal (6°S, 35°W) e de Alcântara (2°S, 44°W), a bordo de foguetes SONDA II e SONDA III. As emissões investigadas foram O_2 275 nm, OI 557.7 nm, Na D 589 nm, OI 630 nm, O_2 761.9 nm e OH (8,3) 724.2 nm. Os resultados destes experimentos, junto com dados obtidos com fotômetros, radar de laser e sondadores ionosféricos, foram utilizados para investigar os mecanismos de excitação e as distribuições verticais dos constituintes minoritários da mesosfera superior e termosfera inferior. Neste artigo apresentamos uma síntese dos resultados destas investigações já publicados na literatura aberta.*

INTRODUÇÃO

Over the past 8 years INPE has carried out a number of rocket-borne experiments aimed at measuring atmospheric airglow emission profiles. These experiments have been carried out in cooperation with the Brazilian Aeronautics and Space Institute (IAE), which has developed the rockets used. Emissions which have been measured are O_2 Herzberg, OI 557.7 nm, Na D 589 nm, OI 630 nm, O_2 A(0,0) 761.9 nm, OH(8,3) 724.4 nm and $O_2(^1\Delta)$ 1.27 μ. Results have been published for the OI 557.7 nm, NaD 589 nm, OI 630 nm and O_2(0,0) 761.9 nm emissions. The experiments carried out so far are summarized in Table 1.

The experiments have used the SONDA II and SONDA III rockets developed by IAE. The SONDA II vehicle is a single stage rocket designed to carry a payload of up to 100 kg to an apogee of about 90 km. This vehicle was used only for the 1991 launch, designed to measure the $O_2(^1\Delta)$ emission. The SONDA III, used in the 1985, 1986 and 1992 experiments, is a two stage vehicle capable of carrying 150 kg to around 500 km. A number of different payload configurations have been used in the experiments. In the first two launches, in 1985 and 1986, the configuration was dictated by the lack of an ejectable nose cone for the SONDA III rocket. In these two experiments the photometers were deployed from the sides of the payload bay, behind the fixed nose cone, as illustrated in Fig. 1. In the 1991 and 1992 experiments a conventional ejectable split nose cone was used. The payload for measuring $O_2(^1\Delta)$, shown in Fig. 2, contained a single infra- red photometer, provided by the University of Saskatchewan. The 1992 experiment, denominated "MULTIFOT" was a much more ambitious payload, containing 6 forward-looking and 4 sidelooking photometers. This payload is shown in Fig. 3.

The photometers used in all the experiments, except for the $O_2(^1\Delta)$ measurement, used the basic layout shown in Fig. 4. 2-inch optics were used in all the photometers, which had acceptance angles between 1 and 3 degrees half-angle. In- flight calibration and dark current measurement were achieved via a motor-driven disc containing a small radioactively excited phosphor light source. The photomultipliers used were operated in the photon-counting mode, with the signal being registered by 12-bit counters in 5 ms time bins. Signals were transmitted at 200 samples per second via a PCM telemetry system. Housekeeping data, such as photomultiplier EHT, filter temperature etc., were telemetered at lower sample rates. The MULTIFOT payload used 4 side-looking photometers in addition to 6 conventional forward-looking instruments of the type illustrated in Fig. 4. The side-looking photometers were basically similar to the longitudinal instruments, with fairly minor modifications to the optics and physical layout, as shown in Fig. 5, so as to enable the photometer to fit inside the 30 cm diameter of the payload bay. All the payloads used 2-axis magnetometers for attitude information.

Except for the 1991 experiment to measure $O_2(^1\Delta)$, all the payloads included electron density probes. The 1985 payload contained a high frequency capacitor probe at the apex of the nose cone, and later launches included combined high frequency capacitor and Langmuir or pulsed plasma probes. These sensors were developed by INPE's ionosphere group, and results have been published elsewhere (see for example, Abdu et al., 1988). The MULTIFOT payload also included an electron temperature probe provided by the Japanese Institute of Space and Astronautical Sciences (ISAS). The 1986 payload was equipped with a number of wide-band (0.3 to 1.1 μ) wide-angle silicon photodiode detectors designed to investigate the strong vehicle glow which was observed in the 1985 experiment.

All the experiments have been conducted at equatorial sites. The 1985 and 1986 launches were from the Barreira do Inferno Launch Center, near to the city of Natal in the state of Rio Grande do Norte,

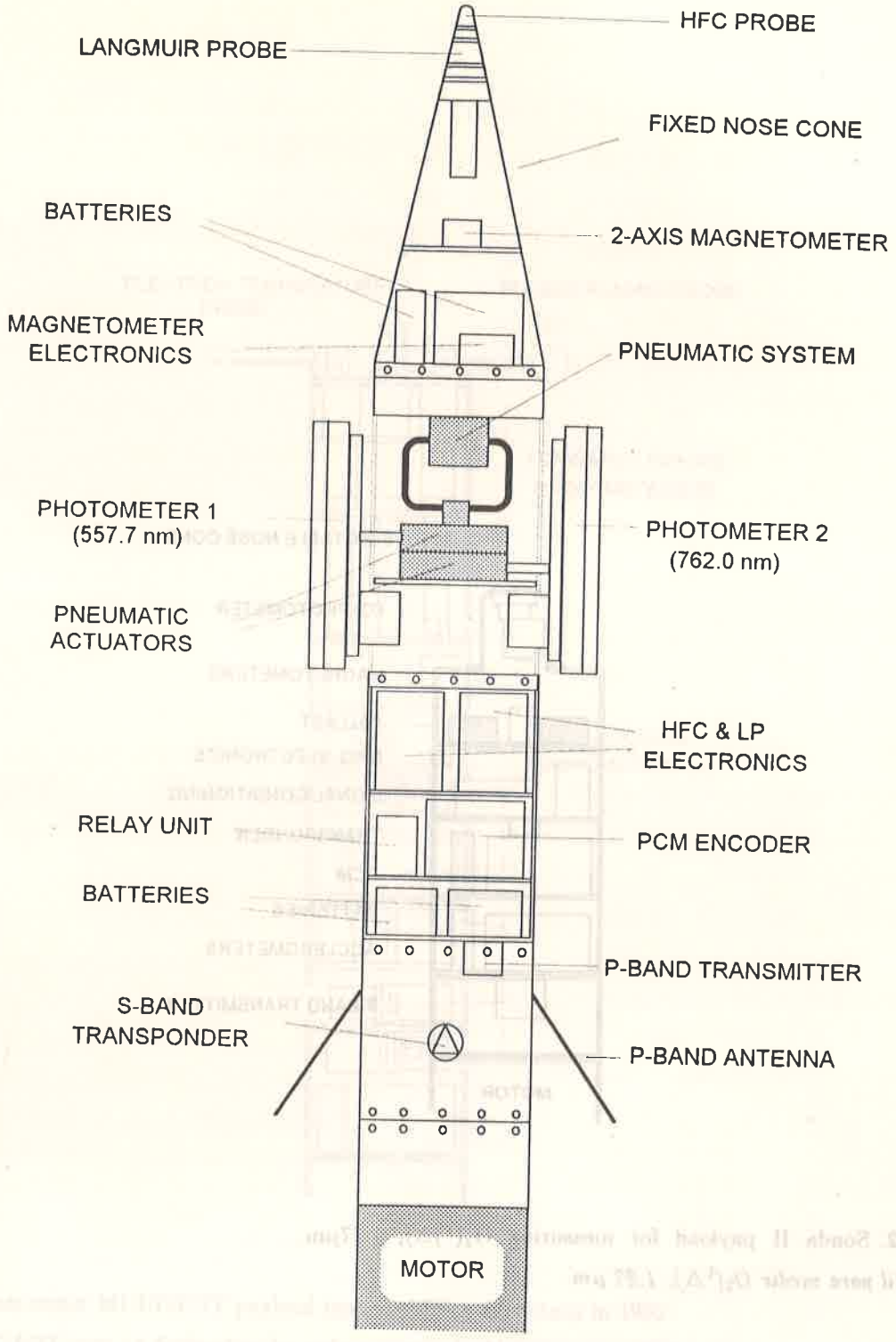

Figure 1. 2-photometer payload of the type launched from Natal in 1985 and 1986.

Carga útil de 2 fotômetros do tipo referente àquela lançada de Natal em 1985 e 1986.

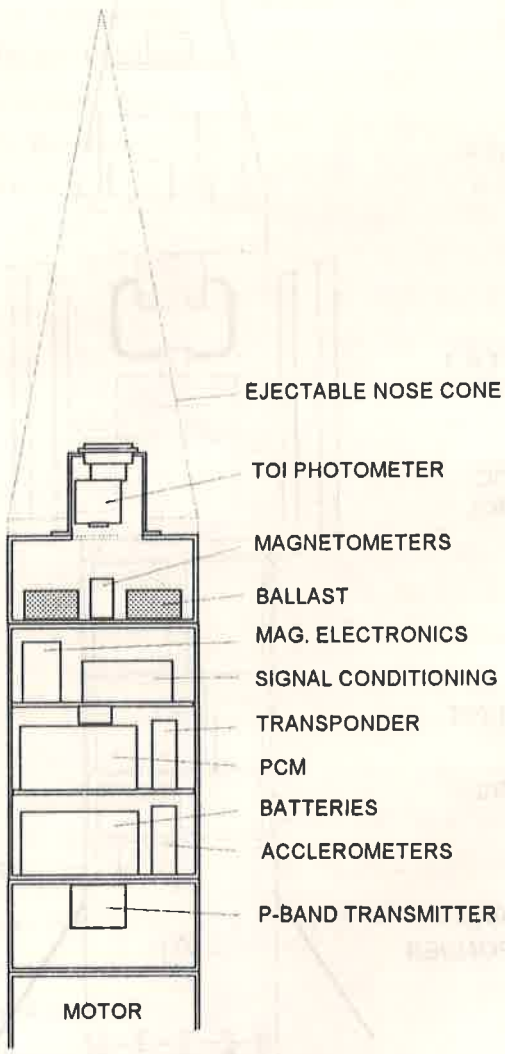

Figure 2. Sonda II payload for measuring $O_2(^1)\Delta)$, 1.27μm.
Carga útil para medir $O_2(^1\Delta)$, 1.27 μm.

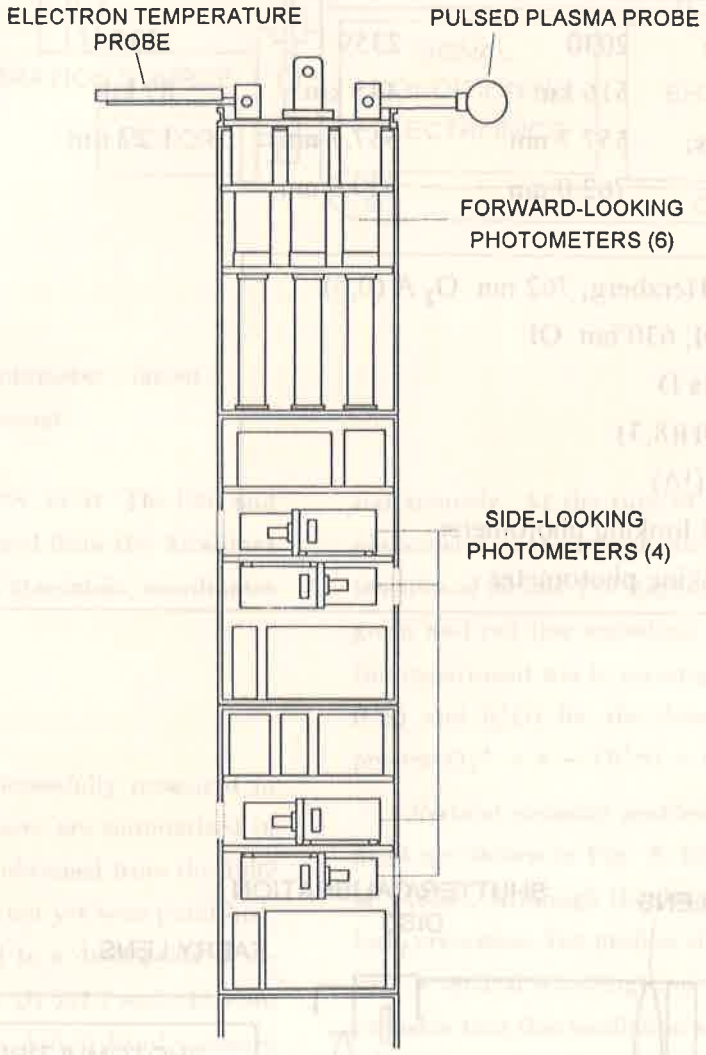

Figure 3. 10-photometer MULTIFOT payload launched from Alcântara in 1992.
Carga útil MULTIFOT com 19 fotômetros lançada a partir de Alcântara em 1992.

Table 1. INPE Rocket-borne airglow experiments.

Experimentos do INPE em luminescência atmosférica a bordo de foguetes.

Date:	**11-12-85**	**31-10-86**	**09-12-91**	**30-05-92**
Local Time:	2030	2359	1830	2352
Apogee:	516 km	445 km	89 km	282 km
Photometers:	557.7 nm	557.7 nm	1.27 μm	275.0 nm (F)
	762.0 nm	630.0 nm		557.7 nm (F)
				578.0 nm (F)
				589.3 nm (F)
				724.2 nm (F)
				762.0 nm (F)
				589.3 nm (S)
				630.0 nm (S)
				713.0 nm (S)
				724.2 nm (S)

275 nm: O_2 Herzberg; 762 nm: O_2 A (0,0)
557.7 nm: OI; 630 nm: OI
589.3 nm: Na D
724.2 nm: OH(8,3)
1.27 μm: $O_2(^1\Delta)$
F = Forward-looking photometer
S = Side-looking photometer

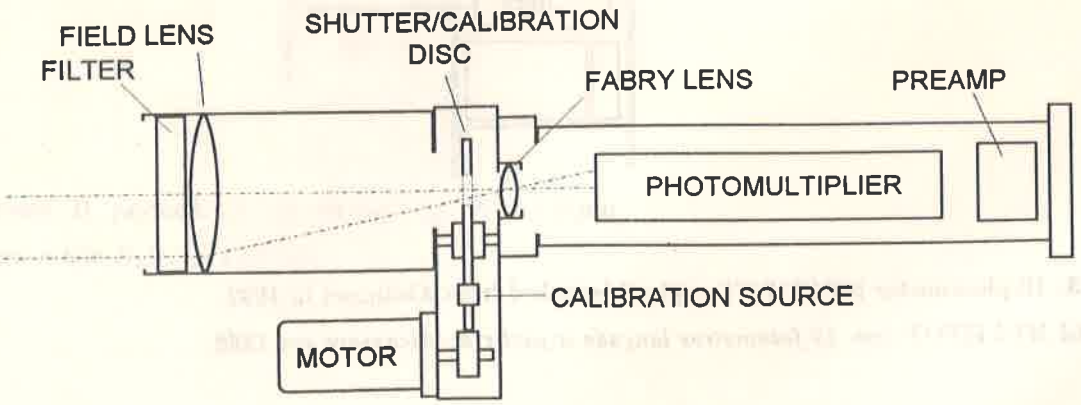

Figure 4. Forward-looking photometer layout.

Fotômetro de visada longitudinal.

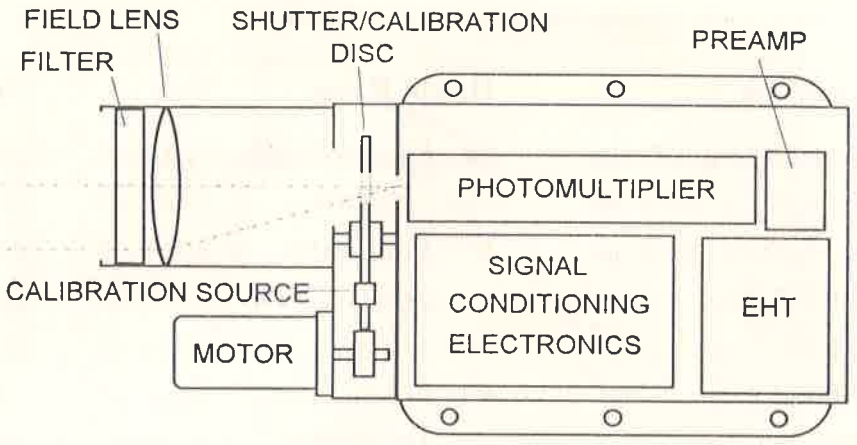

Figure 5. Side-looking photometer layout.
Fotômetro de visada transversal.

with geographic coordinates 6°S, 35°W. The 1991 and 1992 experiments were launched from the Alcântara Launch Center in the state of Maranhão, coordinates 2°S, 44°W.

RESULTS

The emission profiles successfully measured in the experiments described above are summarized in Table 2. Most of the profiles obtained from the 1992 MULTIFOT experiment have not yet been published. This review will be restricted to a description of already published results on the OI 557.7 and 630.0 nm emissions, the 761.9.0 nm O_2 A(0,0) band emission and the sodium doublet.

THE OI 557.7 AND 630.0 nm F-REGION EMISSIONS

In 1986 a 2-photometer payload was launched just before local midnight from the Barreira do Inferno Launch Center under quiet geomagnetic conditions. Ionograms from a nearby site (Fortaleza, 4°S, 38°W) showed a normal development of the equatorial anomaly. At the time of launch a ground-based photometer at the launch site indicated overhead intensities of 90 and 270 Rayleighs respectively for the green and red line emissions. The main purpose of this experiment was to investigate the quantum yields $f(^1S)$ and $f(^1D)$ for the dissociative recombination process $O_2^+ + e \rightarrow O(^1S) + O(^1D)$.

Vertical emission profiles from the 1986 experiment are shown in Fig. 6, taken from Takahashi et al. (1990). Although the data were corrected for vehicle precession, the profiles show a strong oscillation with a vertical wavelength of about 45 km. It seems probable that this oscillation resulted from horizontal structure in the emission layers, not compensated by the correction process. Determination of the quantum efficiencies requires knowledge of electron density, molecular oxygen neutral and ion densities and the atomic oxygen profile. Of these parameters only the electron density was measured simultaneously with the airglow. For this reason Takahashi et al. (1990) limited themselves to a discussion of the ratio of the quantum efficiencies, $\eta = f(^1S)/f(^1D)$. Determination of this ratio requires a knowledge of only the

Table 2. Emission profiles obtained from the experiments shown in Table 1.

Perfis de emissão obtidos nos experimentos mostrados na Tabela 1.

Emission	Height Range	Date	Time
O_2 Herzberg, 275 nm	90 - 110 km (U/D)	31-05-92	2352 LT
O_2 A (0,0), 761.9 nm	90 - 115 km (U)	11-12-85	2030 LT
O_2 A (0,0), 761.9 nm	85 - 110 km (D)	31-05-92	2352 LT
OI 557.7 nm	90 - 115 km (U/D)	11-12-85	2030 LT
OI 557.7 nm	90 - 330 km (U)	31-10-86	2359 LT
OI 557.7 nm	90 - 110 km (U/D)	31-05-92	2352 LT
OI 630.0 nm	90 - 330 km (U/D)	31-10-86	2359 LT
Na D, 589.0 nm	80 - 100 km (U)	31-05-92	2352 LT
OH (8,3), 724.2 nm	80 - 100 km (U)	31-05-92	2352 LT
$O_2(^1\Delta)$, 1.27 μ	60 - 85 km (U)	09-12-91	1812 LT

U = upleg, D = downleg

molecular oxygen and nitrogen profiles, for which realistic models exist. If quenching of $O(^1D)$ by atomic oxygen (Abreu et al., 1986) is taken into account then an atomic oxygen profile must also be assumed.

Takahashi et al's. (1990) vertical profiles of η are shown in Fig. 7. In this figure the profile marked "[L-C]" was calculated using quenching rates from Link and Cogger (1988), and does not include the effects of quenching by atomic oxygen. The curve marked "[ABR]" was calculated using Abreu et al's. (1986) quenching scheme, which includes atomic oxygen quenching. Neutral constituent profiles for these calculations were computed using the MSIS-86 model atmosphere. From Fig. 7 it can be seen that η increases rapidly with height up to about 270 km, equal to the height of the peak of the electron density distribution measured simultaneously, also shown in Fig. 7. Abreu et al. (1983), analyzing data from the visible airglow experiment on board the AE-E satellite, found $f(^1S)$ to increase approximately linearly with the ratio N(e)/N(O), introduced by Bates and Zipf (1980), as a measure of the vibrational excitation of O_2^+. In Fig. 8, Abreu et al's. (1983) AE-E data are plotted together with the quantum yield ratios derived from the rocket experiment as a function of the r parameter, $10^{-4}(T/300)^{-.55}N(e)/N(O)$. There is generally poor agreement between the satellite measurements and the rocket results, the latter giving much smaller values of η than the former. For r values above 10 the rocket measurements indicate that η becomes independent of r, and for r less than 2 η decreases rapidly with r.

A somewhat more speculative analysis of the 1986 results has been published by Sobral et al. (1992). These workers used N_2, O_2, O and T profiles from a model atmosphere, together with what amounts to a simple analytical model for ion composition, to enable them to compute $f(^1S)$ and $f(^1D)$ individually, rather than their ratio. The results which they obtained are shown in Fig. 9. Bates (1992) has pointed to discrepancies between the values shown for $f(^1S)$ in Fig. 8 and theoretical values at heights below 220 km. On the other hand, the experimental measurements must be treated with caution at these heights, because the error introduced by any inaccuracy in correcting for vehicle precession is very large.

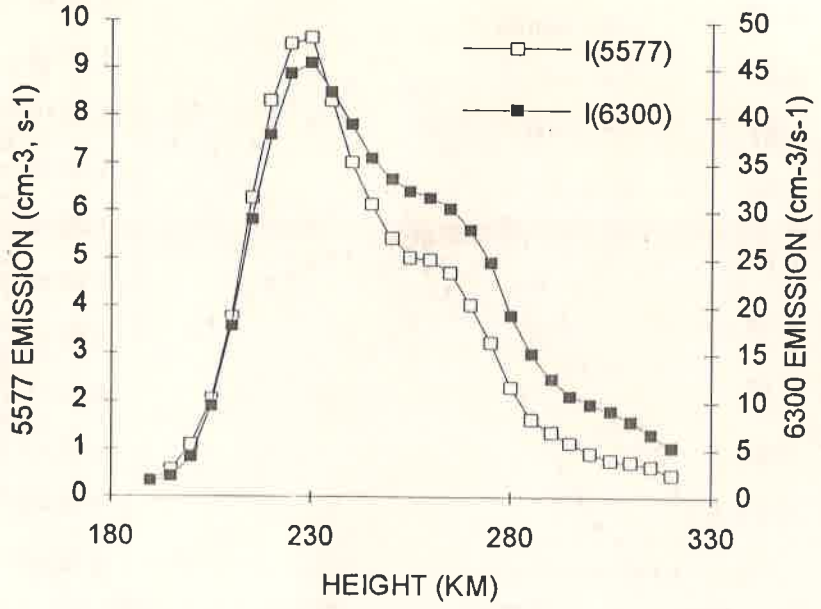

Figure 6. Vertical profiles for OI 557.7 nm and OI 630.0 nm emissions (After Takahashi et al., 1990).
Perfis verticais das emissões de OI 557.7 nm e OI 630 nm. (Segundo Takahashi et al., 1990).

A second discrepancy between the rocket measurements and theoretical quantum yields concerns the increasing values of f(^{1}D) above 250 km. Bates (1992) has suggested that this could result from O(^{1}D) transport by suprathermal atoms. Before this suggestion can be accepted, however, a more careful assessment of the probable systematic error in the f(^{1}D) profile derived from the rocket measurement needs to be carried out. It must not be forgotten that the derivation involves the use of model atmosphere values for most of the parameters involved. Apart from the discrepancies described above, Bates (1992) found good agreement between the rocket measurements and theoretical calculations.

E-REGION OI 557.7 nm AND O_2 A(0,0) 761.9 nm EMISSIONS.

On December 11, 1985, a payload of the type shown in Fig. 1 was used to measure the vertical profiles of the OI 557.7 nm and O_2 A(0,0) 761.9 nm emissions. The payload was launched at 2030 LT from the Barreira do Inferno Launch Center. Good profiles were obtained on the upleg, but unexpected heating of the payload caused excessive thermal noise in the 762 nm photometer during the downleg passage through the emitting region. This problem was avoided in later flights by better thermal insulation of the photometers. At the time of launch the F-region was high, and showed a well developed bubble, so the F region component of OI 557.7 was too small to enable a reliable profile to be obtained. The profiles obtained are shown in Fig. 10, taken from Gobbi (1988). Although the centroid of the O_2 atmospheric band emission profile is slightly lower than that of the OI 557.7, the difference in peak height is surprisingly small.

The two-step energy transfer mechanism originally suggested by Barth (1964) is now well established as being responsible for the green line emission from the E-region. Simultaneous measurements of the airglow and atomic oxygen profiles have been used by McDade et al. (1986) to establish the appropriate quenching parameters. Gobbi et al. (1992) have used McDade et al's. parameters to calculate atomic

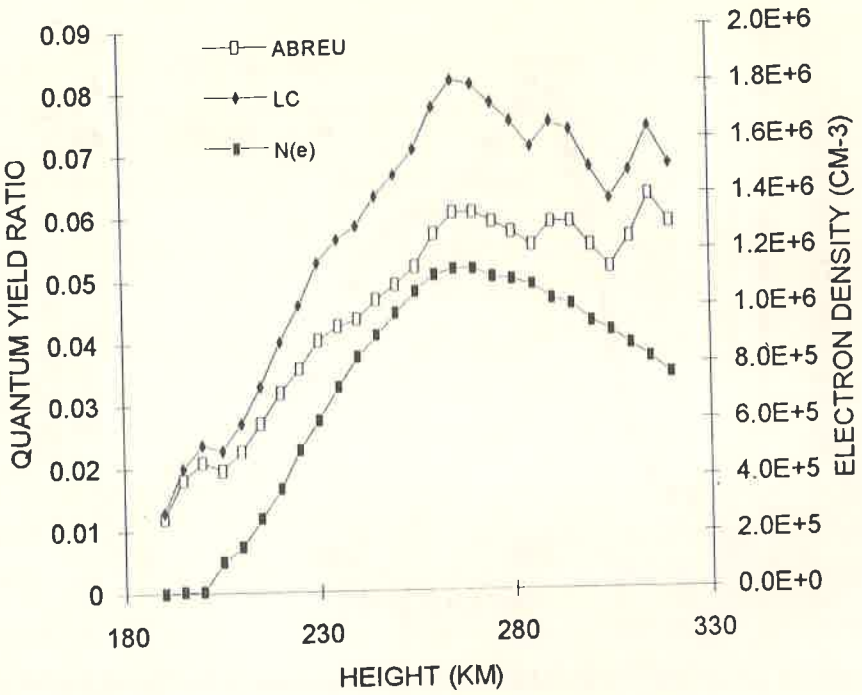

Figure 7. Ratio of the quantum yields $f(^1S)/f(^1D)$ as a function of height. (After Takahashi et al., 1990).

Razão entre as eficiências quânticas $f(^1S)/f(^1D)$ em função de altura. (Segundo Takahashi et al., 1990).

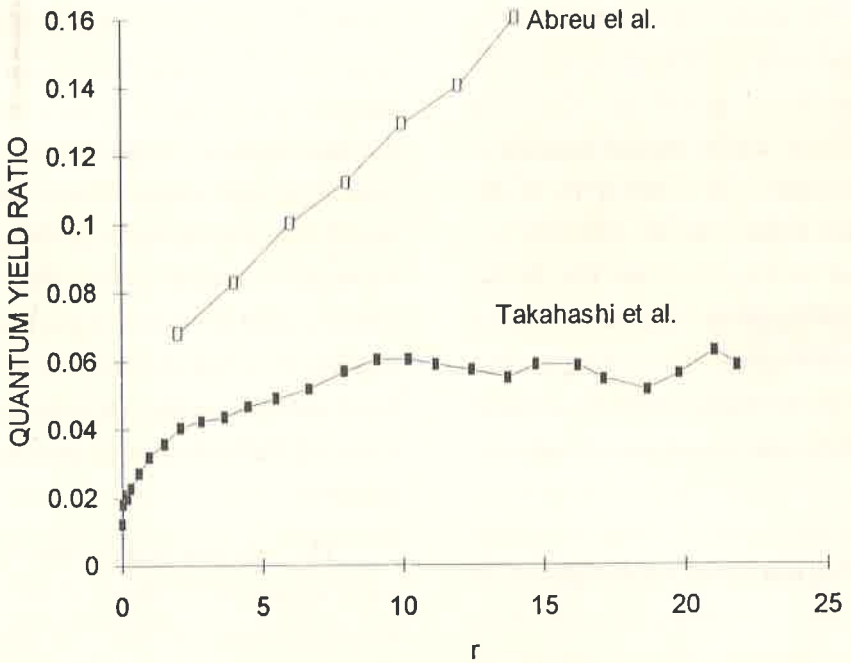

Figure 8. Quantum yield ratios as a function of the r parameter, $10^{-4}(T/300)^{-55}N(e)/N(O)$. (After Takahashi et al., 1990).

Razão entre as eficiências quânticas em função do parâmetro r, $10^{-4}(T/300)^{-55}N(e)/N(O)$. (Segundo Takahashi et al., 1990).

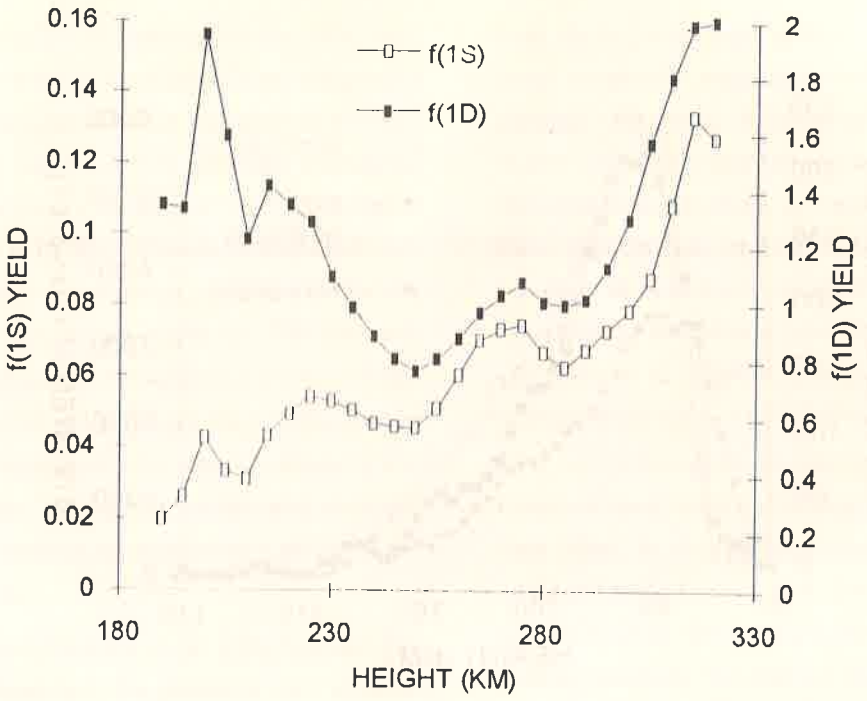

Figure 9. Quantum yields f(^{1}S) and f(^{1}D) as a function of height. (After Sobral et al., 1992).
Eficiências quânticas f(^{1}S) e f(^{1}D) em função de altura. (Segundo Sobral et al., 1992).

oxygen profiles from the 1985 and 1986 OI 557.7 nm emission profiles measured at Natal. The results of this analysis are shown in Fig. 11. The difference between the upleg and downleg profiles for the 1985 experiment indicates the existence of large horizontal gradients in atomic oxygen. Gobbi et al. (1992) point to the fact that the OI 557.7 nm zenith intensity measured by a ground based photometer was decreasing rapidly at the time of the experiments, indicating the existence of strong gradients in both space and time.

THE Na D LINE EMISSION

The sodium doublet nightglow emission has received very little attention, probably because its source is generally considered to be well understood. The reaction sequence Na + O_3→ NaO + O_2; NaO + O →Na* + O_2, suggested by Chapman (1939) is believed to be responsible for the production of the Na(^{2}P) which gives rise to the sodium doublet in the nightglow. The fact that calculations of the expected total zenith intensities, on the basis of typical measured ground-state sodium distributions and ozone profiles, using laboratory rate coefficients, gave values 2 orders of magnitude too low has been largely ignored. Fortunately, however, recent work by Herschbach et al. (1992) appears to have resolved this discrepancy. On the other hand, despite the existence of very extensive lidar measurements of the ground-state sodium distribution, no simultaneous measurement of the emission profile has been reported hitherto. Ideally, of course, a simultaneous measurement of ground-state sodium, Na D emission rate and ozone density would enable a full test of the theory. In the 1992 MULTIFOT experiment a lidar installed at the launch site was used to measure the vertical distribution of ground-state sodium simultaneously with the airglow profile. Ozone was not measured.

Considerable care must be taken in measuring the Na D emission profile because the emission intensity is typically weak, and the 589 nm photometer will also respond to the NO_2 continuum and the OH(8,2)

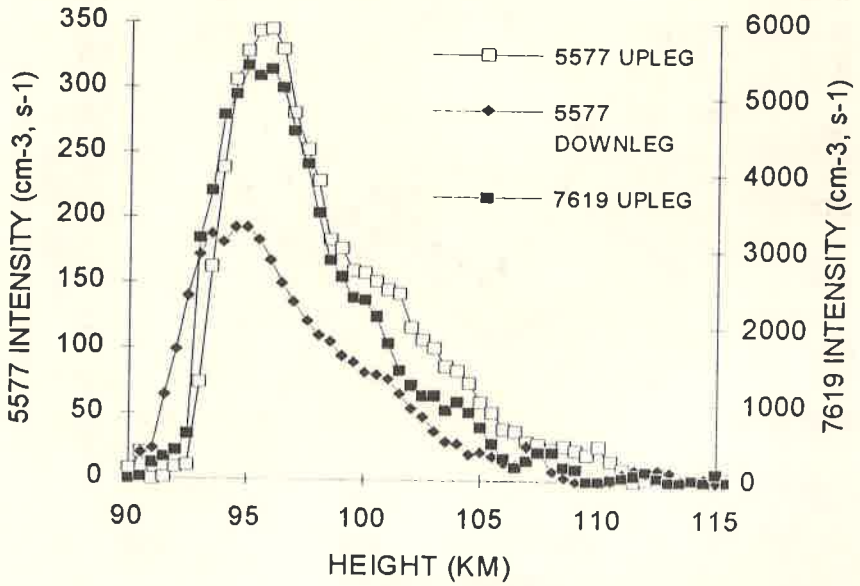

Figure 10. OI 557.7 nm and O_2 A(0,0) 761.9 nm vertical emission profiles. (After Gobbi, 1988).

Perfis verticais das emissões OI 557.7 nm e O_2 A(0,0) 761.9 nm. (Segundo Gobbi, 1988).

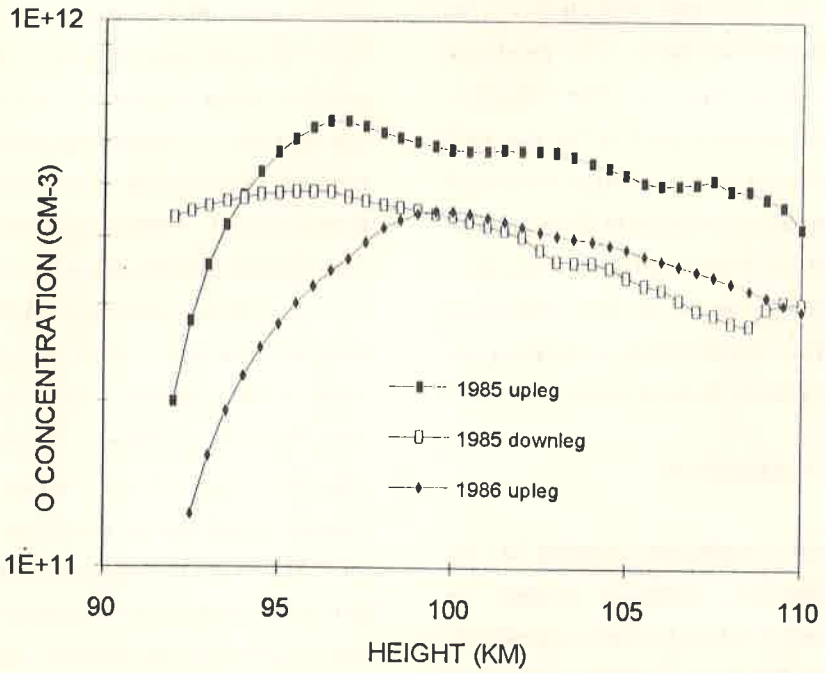

Figure 11. Vertical distribution of atomic oxygen derived from OI 557.7 emission profiles. (After Gobbi et al., 1992).

Distribuição vertical de oxigênio atômico derivada do perfil da emissão de OI 557.7 nm. (Segundo Gobbi et al., 1992).

band. In the MULTIFOT experiment the NO_2 continuum was allowed for on the basis of the background signal measured by a photometer centered on 578 nm, and the OH(8,2) band contribution was calculated from the simultaneously measured OH(8,3) emission at 724.2 nm. The MULTIFOT payload included both forward-looking and side-looking photometers for Na D, OH (8,3) and background emissions. The forward-looking infrared photometers suffered serious contamination effects on the upleg, where the profiles should be most directly comparable to measurements by the ground-based lidar, so the OH profile was obtained by inverting the horizon intensities seen by the side-looking instrument.

Fig. 12, from Clemesha et al. (1993) shows the simultaneously measured Na emission and ground-state sodium profiles. The most interesting characteristic of Fig. 12 is the remarkable similarity between the profiles. The small difference in the height of the bottomside of the layers could well be caused by a small horizontal gradient between the lidar site and the point at which the payload passed through the emission layer, separated by about 60 km. The radiative lifetime of $Na(^2P)$ is extremely short, so it can be assumed that the emission intensity should be proportional to the product of the ground-state sodium and ozone concentrations. Thus the results shown in Fig. 11 imply an almost constant ozone density from about 85 km to almost 100 km. There is not a great deal of experimental data on ozone above 90 km, but it would certainly be expected that its concentration should fall rapidly in this region. The direct proportionality between airglow intensity and ground-state sodium concentration, which Fig. 12 appears to demonstrate, inevitably raises questions with respect to the validity of the Chapman mechanism.

VEHICLE GLOW

Rocket measurements of airglow emissions almost invariably suffer from contamination glow effects during some part of the rocket trajectory. The most commonly suggested cause for such effects is payload outgassing. A curiosity of the 1985 and 1986 flights is that they showed contamination effects quite different from anything previously reported. In both these experiments, at heights below 87 km, the photometers showed contamination signals strongly modulated at the rocket spin rate. Figures 13 and 14, from Clemesha et al. (1987) show samples of the contamination observed in the 1985 experiment. From Fig. 14 it can be seen that the signals seen by the two photometers were exactly 180 degrees out of phase with each other. In the 1986 experiment 2 wide band, wide angle photodiode detectors also monitored the glow, one looking in the forward direction and the other looking towards the rear of the vehicle. While the forward-looking photodiode registered contamination signals similar to those seen by the airglow photometers, the backward-looking detector was saturated up to 80 km, after which height the signal fell to zero within a few km, without showing spin modulation.

The comparative magnitudes of the total intensities seen by the forward-looking wide band detector and the airglow photometers suggest that the contamination glow was wide band. The height variation of the contamination signals is shown in Fig. 15, from Clemesha et al. (1988). It can be seen that the shorter wavelength signals tend to fall off more rapidly with height than those seen by the longer wavelength photometers, and that the e-folding distance for the intensities is much smaller than the atmospheric scale height. On the basis of this information it was concluded that the contaminating signals were produced by vehicle glow in the shock wave around the nose cone, the singular nature of the signals being a result of the unusual configuration of the payload combined with the exceptionally high velocity (about 2.7 km/s) of the vehicle at the heights in question.

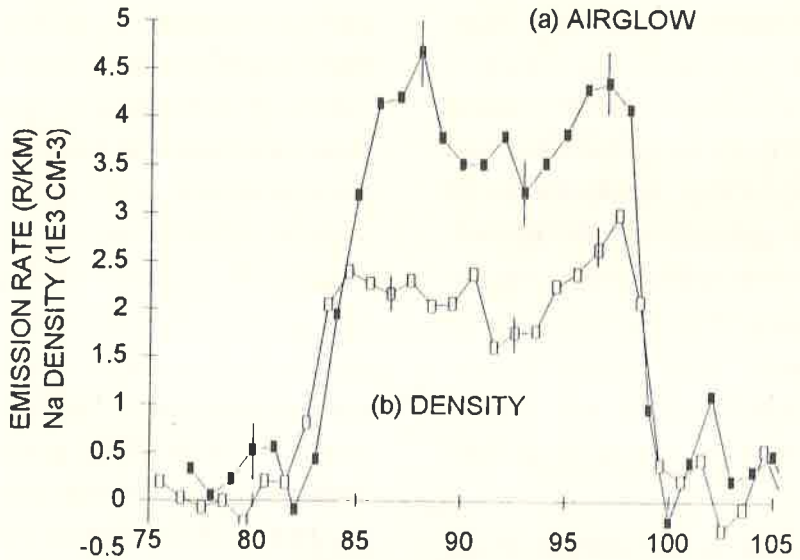

Figure 12. Vertical profiles of ground state sodium and Na D emission intensity measured simultaneously. (After Clemesha et al., 1993).

Perfis verticais de sódio no estado terra e da intensidade da emissão Na D, obtidos simultaneamente. (Segundo Clemesha et al., 1993).

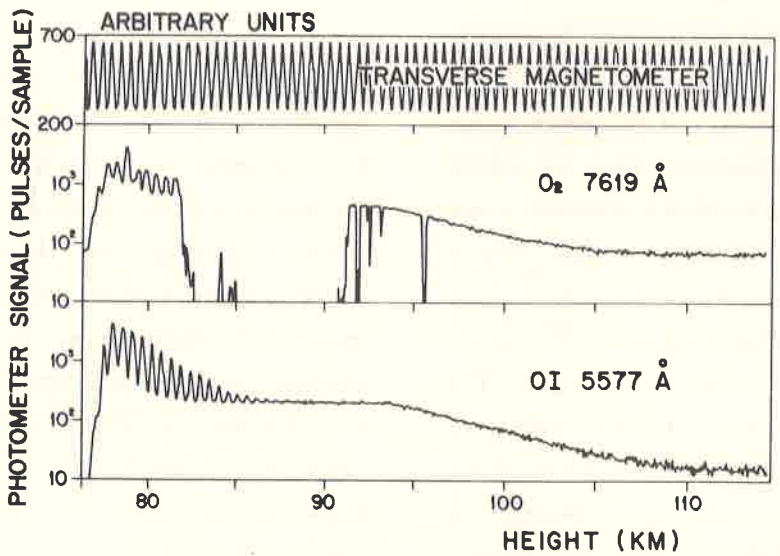

Figure 13. Vehicle glow observed during the upleg of the 1985 experiment. (After Clemesha et al., 1987).

Luminescência veicular observada durante a subida do experimento de 1985. (Segundo Clemesha et al., 1987).

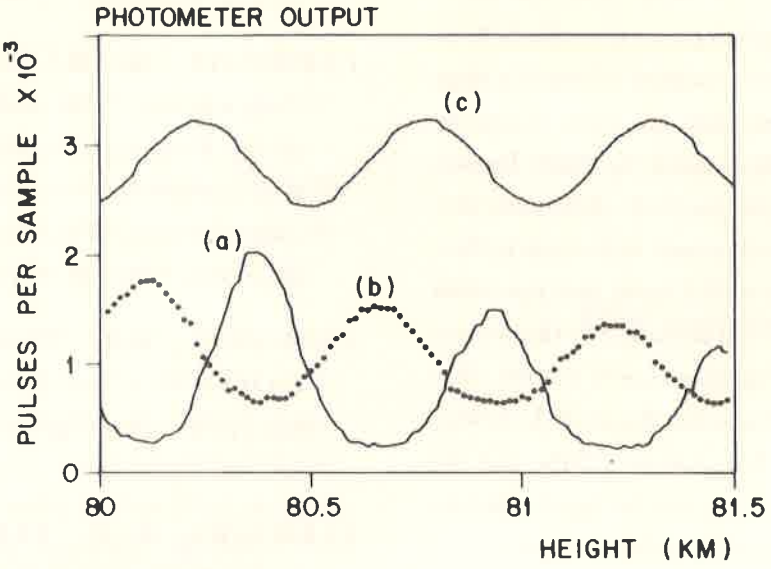

Figure 14. Phase relationship between vehicle glow observed by the 2 photometers of the 1985 flight. (After Clemesha et al., 1987).

Relação de fase entre os sinais de luminescência veicular observados nos 2 fotômetros do experimento de 1985. (Segundo Clemesha et al., 1987).

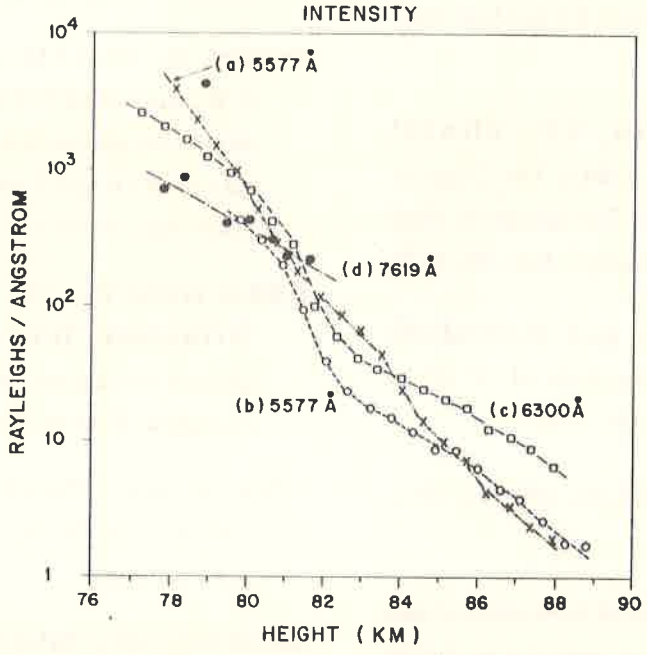

Figure 15. Height variation in the intensity of vehicle glow for various wavelengths. (After Clemesha et al., 1988).

Variação com altura da intensidade de luminescência veicular em vários comprimentos de onda. (Segundo Clemesha et al., 1988).

ACKNOWLEDGEMENTS

INPE's rocket-borne airglow experiments have been made possible by the combined efforts of a large number of people. A key role has been played by Agnaldo Eras who, ably assisted by Narli Baesso, has designed most of the payload electronics and coordinated payload development and construction. Thanks are also due to the IAE team that has taken care of vehicle-payload integration, and to the personnel of the Natal and Alcântara launch centers. Research grants from the Conselho Nacional de Desenvolvimento Científico e Tecnológico - CNPq, and the Fundação de Amparo à Pesquisa do Estado de São Paulo - FAPESP are gratefully acknowledged.

REFERENCES

ABDU, M. A., MURALIKRISHNA, P., BATISTA, I.S. and CHAVES, A.H.P. (1988) On the rocket-induced wave disturbances in the daytime equatorial ionosphere, J. Geophys. Res., 93, 2758.

ABREU, V. J., SOLOMON, S.C., SHARP, W.E. and HAYS, P.B. (1983) The Dissociative Recombination Of O_2^+: The Quantum Yield of $O(^1S)$ and $O(^1D)$, J. Geophys. Res., 88, 4140.

ABREU, V.J., YEE, J.H. and SOLOMON, S.C. (1986) The Quenching Rate of $O(^1D)$ by $O(^3P)$, Planet. Space Sci., 34, 1143.

BARTH, C.A. (1964) Three-body reaction, Ann. Geophys., 20, 182.

BATES, D.R. (1992) Emission of forbidden red and green lines of atomic oxygen from the nocturnal F region, Planet. Space Sci., 40, 893.

BATES, D.R. and ZIPF, E.C. (1980) The $O(^1S)$ quantum yield from O_2^+ dissociative recombination, Planet. Space Sci., 28, 1081.

CHAPMAN, S. (1939) Notes on atmospheric sodium, Astrophys. J., 90, 309.

CLEMESHA, B. R., SIMONICH, D.M., TAKAHASHI, H. and MELO, S. M.L. (1993) A simultaneous measurement of the vertical profiles of sodium nightglow and atomic sodium density in the upper atmosphere, Geophys. Res. Lett., 20, 1347.

CLEMESHA, B.R., TAKAHASHI, H. and SAHAI, Y. (1987) Vehicle glow observed during a rocket sounding experiment, Planet. Space Sci., 35, 1367.

CLEMESHA, B. R., TAKAHASHI, H. and SAHAI, Y. (1988) Contamination glow observed during two rocket sounding experiments, Progress in Atmospheric Physics, Kluwer Academic Publishers, 109.

GOBBI, D. (1988) M. S. dissertation, Instituto Nacional de Pesquisas Espaciais.

GOBBI, D., TAKAHASHI, H., CLEMESHA, B.R. and BATISTA, P.P. (1992) Equatorial atomic oxygen profiles derived from rocket observations of OI 557.7 nm airglow emission, Planet. Space Sci., 40, 775.

HERSCHBACH, D. R., KOLB, C. E., WORSNOP, D.R. and SHI, X. (1992) Excitation mechanism of the mesospheric sodium nightglow, Nature, 356, 414.

LINK, R. and COGGER, L.L. (1988) A reexamination of the OI 6300-Å nightglow, J. Geophys. Res., 93, 9883.

McDADE, I.C., MUSTAGH, D.P., GREER, R.G.H., DICKINSON, P.H.G., WITT, G., STEGMAN, J., LLEWELLYN, E.J., THOMAS, L. and JENKINS, D.B. (1986) ETON 2: quenching paramenters for the proposed precursors of $O_2(\Sigma_g^+)$ and $O(^1S)$ 557.7 nm

in the terrestrial nightglow, Planet. Space Sci., 34, 789.

SOBRAL, J.H.A., TAKAHASHI, H., ABDU, M.A., MURALIKRISHNA, P. and ZAMLUTTI, C.J. (1992) O(^{1}S) and O(^{1}D) quantum yields from rocket measurements of electron densities and 557.7 and 630 nm emissions in the nocturnal F-region, Planet. Space Sci., 40, 607.

TAKAHASHI, H., CLEMESHA, B.R., BATISTA, P.P., SAHAI, Y., ABDU, M.A. and MURALIKRISHNA, P. (1990) Equatorial F-Region OI 6300 Å and OI 5577 Å Emission Profiles Observed by Rocket-Borne Airglow Photometers, Planet. Space Sci., 38, 547.

ZIPF, E.C. (1988) The excitation of the O(^{1}S) state by the dissociative recombination of O_2^+ ions: electron temperature dependence, Planet. Space Sci., 36, 621.

Submetido em 16.08.93
Revisado em 06.09.93
Aceito 10.09.93
Editor responsável V.W.J.H. Kirchhoff

Palavras chave	**Key words**
Oxigênio	Oxygen
Foguete	Rocket
Luminescência	Airglow